REMOTE SENSING OF H IN LUNAR SURFACE MATERIALS: THE EFFECT OF COMPOSITION ON HYDROGEN SOLUBILITY AND QUANTIFICATION. M. D. Dyar[1], K. A. Hibbitts[2] P. L. King[3], E. A. Breves[1,] T. M. Orlando[4], M. J. Poston[4], G. A. Grieves[4], J. M. Tucker[5], and S. J. Seaman[6].[1]Dept. of Astronomy, Mount Holyoke College, South Hadley, MA 01075, mdyar@mtholyoke.edu; [2]Johns Hopkins University, Applied Physics Laboratory, Laurel, MD, 20723; [3]Research School of Earth Sciences, Australia National University, Canberra, ACT, 0200; [4]Georgia Institute of Technology, Atlanta, GA, 30332; [5]Dept. of Earth and Planetary Sciences, Harvard University, Cambridge, MA 02138; [6]Dept. of Geosciences, University of Massachusetts, Amherst, MA 01003.

Introduction: It is now well-known that three different missions have definitely detected evidence for the presence of OH^{-1} on the lunar surface [1-3]. This paper explores the relationship between 3-μm band strength and the composition of lunar surface materials through transmission FTIR spectroscopy of a suite of synthetic lunar-analog glasses.

Sources of H and its Host: Two types of space weathering that produce exogenic H on the lunar surface include infall of meteorite and cometary material containing water or hydroxyl and processes associated with the irradiation by the solar wind. These have the combined effect of both producing significant quantities of impact-created glass (agglutinates in lunar soils) and breaking down the outermost surfaces and crystal structures of minerals. The result is that the outermost nms of lunar surface materials are predominantly amorphous materials, riddled with structural defects such as dangling bonds. The extent to which lunar surface materials can accommodate H depends both on the availability of defects, which create sites for H to reside, and on composition.

Why Does Composition Matter? The basic structural unit of silicate minerals and glasses is the SiO_4 tetrahedron, which forms strongly-bonded networks when all four corners of the tetrahedra are shared. Cation substitutions affect that network by creating "non-bridging" O^{2-} anions that provide sites where H may reside. For example, the addition of alkali cations with low charge and large ionic radii changes bond lengths and bond strengths, not to mention other fundamental properties such as thermal expansion coefficient [see 4], fluidity (inverse of viscosity), diffusion, electrical conduction, and chemical corrosion. Studies of glass structure show that fundamental properties of the glass are thus related to the ratio of network-forming cations (Si^{4+}, Al^{3+}) to network modifiers (especially Na^{+}, and to a lesser extent, K^{+} and Ca^{2+}).

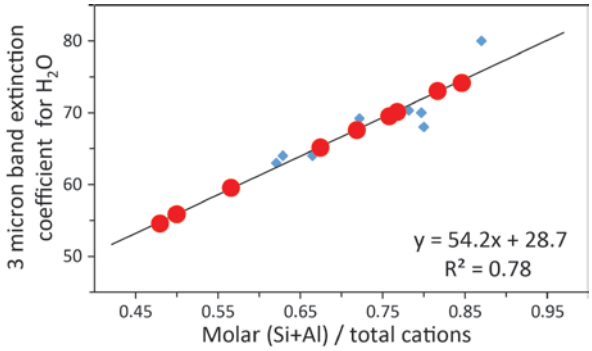

Figure 1.Relationship between glass composition and extinction coefficient based on data summarized in [4].

To determine the H content of amorphous materials using transmission IR, we apply the Bouguer-Beer-Lambert calculation of molar concentration (A / $d\rho\varepsilon$, where A is IR absorbance peak height, d is sample thickness, ρ is density, and ε is the extinction coefficient). Fortunately, ε for the 3 μm band is known for a wide range of compositions. A relationship exists between ε and the ratio of network-forming cations to total cations in a glass (Fig. 1), expressed as (Si+Al)/total cations. This demonstrates the first-order effect of bulk composition on the magnitude of absorption features due to H.

Relating transmission calibrations for H in amorphous materials to reflectance and emis-

Table 1. Glass Compositions Studied and Calculated Extinction Coefficients (ε)

Sample	K-2296	K-2295	K-2294	K-2289	K-2292	82-70	85-3	83-59	85-43
SiO_2	45.50	46.10	46.26	50.19	44.97	56.50	61.20	65.28	68.89
TiO_2	0.40	1.60	0.98		0.30	0.67	0.68	0.49	0.29
Al_2O_3	7.90	14.30	12.98	13.45	26.74	16.60	16.22	16.70	14.64
FeO	5.59	3.15	4.26	0.00	1.23	2.91	2.03	1.68	1.63
Fe_2O_3	15.20	11.71	16.78	0.00	3.89	3.65	2.65	1.87	0.97
MnO						0.12	0.09	0.06	0.07
MgO	17.20	12.50	6.47	14.17	6.86	6.00	4.18	2.55	0.47
CaO	8.60	10.40	12.73	22.19	15.64	8.23	6.56	5.23	1.79
Na_2O		0.80	0.29		0.23	3.16	4.06	4.66	6.00
K_2O		0.10	0.04		0.05	1.48	1.03	1.50	2.74
P_2O_5						0.11	0.23	0.12	0.09
H_2O	0.36	0.47	0.66	0.49	0.20	n.a.	1.44	0.31	1.24
Total	100.75	101.13	101.45	100.49	100.11	99.44	100.37	100.45	98.82
(Si+Al)/total cats	0.49	0.55	0.56	0.56	0.66	0.67	0.72	0.76	0.79
$\%Fe^{3+}$	71	77	78	0	74	53	54	50	35
ε	**55.2**	**58.4**	**59.2**	**59.3**	**64.2**	**65.2**	**67.9**	**69.8**	**71.6**

sion IR obtained during remote sensing will require further development, because such experiments have not yet been performed. However, theory indicates that the ε parameter for transmission spectroscopy may be related to the *k* parameter used in reflectance spectroscopy along with *n*, which is usually constant in the NIR, using the Kramers-Kronig transform [see 9]. Use of appropriate values of ε or *k* (for absorption vs. reflectance measurements), will in any case require assumptions or direct knowledge of the composition of the glass or mineral being studied.

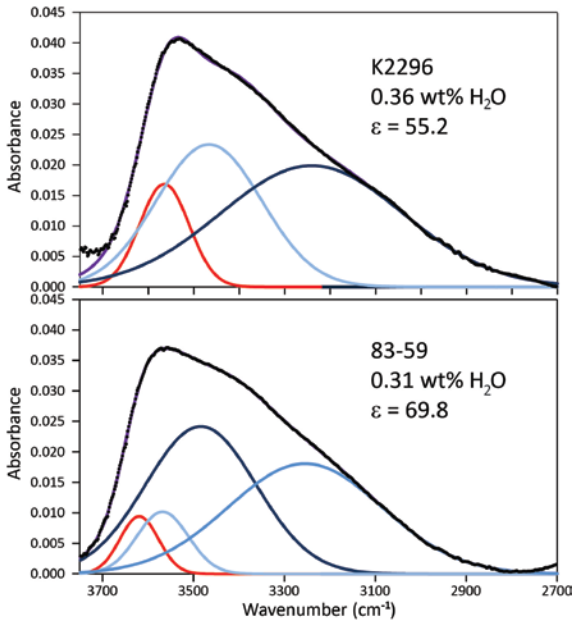

Figure 2. Comparison of the baseline-subtracted 3-μm feature in transmission FTIR spectra of two different glasses of the same thickness with (Si+Al)/total cations = 0.49 (top) and 0.76 (bottom).

Samples and Methods. For this study, we use a suite of lunar-analog synthetic glasses made at Corning glass in two different batches by Daniel Nolet and Gerald Fine (Table 1). All samples were created as large boules (3000-10,000 g) and were synthesized in air. Fe^{3+} was measured using Mössbauer spectroscopy. H contents were quantified using transmission spectroscopy on doubly-polished 30-50 mm thick slices of each glass, coefficients from Table 1, and the Bouguer-Beer-Lambert calculation.

Results and Discussion. Transmission FTIR data of our suite of glasses highlight several important points. Fig. 2 compares two glasses with significantly different compositions: K2296 is a high-Fe, relatively low Si basalt-analog glass. The 83-59 sample is low-Fe and high-Si and alkalis, analogous to anorthositic glass. As a result of these compositional differences, the ratios of (Si+Al)/total cations are quite different: 0.49 and 0.76, respectively. The total area of the 3 μm feature is 19.1 for K2296 and 17.4 for 83-59, in units of absorbance per wavenumber. Although those areas are different, the fact that the ε values (from Fig. 1) are

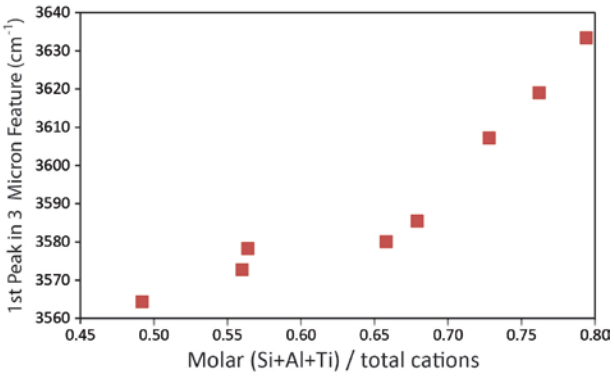

Figure 3. Position of the highest energy peak centroid fit to each glass spectrum as a function of composition, expressed as (Si+Al+Ti)/total cations. Ti is included with Si and Al for this plot because it is significant in lunar compositions.

55.2 and 69.8 for those compositions means that these glasses have nearly the same calculated H_2O contents.

These two glasses also have characteristic peak *shapes*, as do all samples studied, that likely relate directly to composition. For example, fits of individual components to the 3-μm feature show that highest energy component peak fit to lower Si (basaltic) glasses tends to fall at a lower wavenumber than in high-Si glasses (e.g. positions of the red peaks in Fig. 2 are plotted vs. composition in Fig. 3). Samples with similar Si tend to have similar component peaks. Peak positions are fairly consistent among most samples studied, suggesting that the same fundamental vibrations occur across all the compositions but with varying intensities. Thus composition affects not only ε, but also the overall shape of the 3-μm feature. Related work has also shown that it may be possible to use the 10-μm band position to estimate extinction coefficients and better constrain the glass composition [e.g., 5,6]. This raises the likelihood that the shape and position of the 3 μm feature (and possibly other bands) can be used to understand glass composition of lunar surface materials using remote sensing.

Acknowledgments. We thank Jennifer Blank for providing the glass samples made by Gerry Fine. We are grateful for support from the NASA NLSI grants NNA09DB31A, NNA09DB34A, and LASER grant NNX08AZ01G.

References: [1] Clark R. N. (2009) *Science*, 326, 562-564. [2] Pieters C. M. et al. (2009) *Science*, 326, 568-572. [3] Sunshine J. et al. (2009) *Science*, 326, 565-568. [4] King P. L. et al. (2004) *Mineral. Asssoc. Canada, Short Course Series*, 33, 93-133. [5] Lee R. J. et al. (2010) *JGR Solid Earth*, 115, B06202. [6] Dufresne C. D. M. et al. (2009) *Amer. Mineral.*, 94, 1580-1590.